

# Optimization of iron oxide nanoparticles for MRI-guided magnetic hyperthermia tumor therapy: reassessing the role shape in their magnetocaloric effect.

José M. Paez-Muñoz<sup>1,2,†</sup>, Francisco Gámez<sup>3,†</sup>, Yilian Fernández-Afonso<sup>4,5</sup>, Roberto Gallardo<sup>2</sup>, Manuel Pernía Leal<sup>6</sup>, Lucía Gutiérrez<sup>4,5</sup>, Jesús M. de la Fuente<sup>4,7</sup>, Carlos Caro<sup>1,2,\*</sup>, Maria L. García-Martín<sup>1,2,7,\*</sup>.

<sup>1</sup>Biomedical Magnetic Resonance Laboratory-BMRL, Andalusian Public Foundation Progress and Health-FPS, Seville, Spain

<sup>2</sup>Instituto de Investigación Biomédica de Málaga y Plataforma en Nanomedicina (IBIMA Plataforma BIONAND), C/ Severo Ochoa, 35, 29590 Málaga, Spain.

<sup>3</sup>Departamento de Química Física, Facultad de Ciencias Químicas. Universidad Complutense de Madrid, 28040 Madrid, Spain

<sup>4</sup>Instituto de Nanociencia y Materiales de Aragón (INMA), CSIC-Universidad de Zaragoza, 50009 Zaragoza, Spain.

<sup>5</sup>Departamento de Química Analítica, Universidad de Zaragoza, C/ Pedro Cerbuna 12, 50009, Zaragoza, Spain

<sup>6</sup>Departamento de Química Orgánica y Farmacéutica, Facultad de Farmacia, Universidad de Sevilla, C/ Profesor García González 2, 41012 Seville, Spain.

<sup>7</sup>Biomedical Research Networking Center in Bioengineering, Biomaterials & Nanomedicine (CIBER-BBN).

\* email: [ccaro@ibima.eu](mailto:ccaro@ibima.eu) / [mlgarcía@ibima.eu](mailto:mlgarcía@ibima.eu)

## Index

### 1. Methods

- A) Synthesis of Iron Oleate
- B) Development of the custom-made temperature controller
- C) Synthesis of PEGylated ligand
- D) Ligand exchange process
- E) Nuclear Magnetic Resonance Spectroscopy (NMR)
- F) Inductively Coupled Plasma High-Resolution Mass Spectroscopy (ICP-HRMS).
- G) Dynamic Light Scattering (DLS)
- H) Magnetic Characterization
- I) Hyperthermia equipment.
- J) *In vitro* longitudinal relaxivities ( $r_1$ )
- K) Cytotoxicity evaluation
- L) Magnetic Resonance Imaging (MRI) studies
- M) Histology

### 2. Results

- A) Characterization
- B) *In vitro* transverse relaxivity.
- C) Cytotoxicity evaluation
- D) Biodistribution MRI studies in tumor-bearing mice after I.V. administration
- E) MRI of magnetic hyperthermia process
- F) Histology

## 1. Methods

### A) Synthesis of Iron Oleate

A mixture of 10.8 g of iron chloride (40 mmol) and 36.5 g of sodium oleate (120 mmol) was dissolved in 80 ml of ethanol, 60 ml of distilled water and 140 ml of hexane. The resulting solution was heated to 60 °C and left for 4 h allowing a reflux of hexane and in inert atmosphere. At that time, the reaction was cooled down to room temperature and two phases can be distinguished: a lower aqueous phase and an upper organic phase containing the iron oleate. The organic phase was washed 3 times with distilled water and the hexane was evaporated in the rotavapor.

### B) Development of the custom-made temperature controller

```
/* TEMPERATURE RAMP GENERATOR FOR THERMO-STIRRING PLATES IKA  
C-MAG HS */
```

```
#include <stdio.h>
```

```
#define salida8 8
```

```
#define pin9 9
```

```
int tini = 0;
```

```
int tmax = 0;
```

```
int tpor = 0;
```

```
int tpop = 0;
```

```
int tmax2 = 0;
```

```
int toff = 0;
```

```
float tvar = 0;
```

```
float seg = 0;
```

```
float sep = 0;
```

```
float tpp = 0;
```

```
float paus = 0;
```

```

int pulsos = 0;

int suma = 0;

int i = 0;

#define DEBUG(a) Serial.println(a);

void setup()

{

Serial.begin(9600);

Serial.setTimeout(50);

pinMode(salida8, OUTPUT);

digitalWrite(salida8, HIGH);

Serial.print("Enter... [ START TEMP - END TEMP - TIME (min) ]");

}

void loop()

{

if (Serial.available())

{

scanf("%d", tini);

Serial.println();

Serial.print("Start Temperature : ");

tini = Serial.parseInt();

Serial.println(tini);

scanf("%d", tmax);

Serial.print("Max Ramp Temperature : ");

```

```
tmax = Serial.parseInt();

Serial.println(tmax);

Serial.print("Ramp Time : ");

tpor = Serial.parseInt();

Serial.println(tpor);

Serial.print("Pause Time : ");

tpop = Serial.parseInt();

Serial.println(tpop);

Serial.println();

Serial.print("^Temperature = ");

tvar = (tmax - tini);

Serial.println(tvar);

tpp = (tvar / tpor);

Serial.print("Pulse Time = ");

Serial.println(tpp);

Serial.print("Seconds between pulses = ");

sep = (60/tpp);

Serial.println (sep);

Serial.print("Total pulses = ");

pulsos = (tvar);

Serial.println (pulsos);

seg = (sep*1000);

while (pulsos > 0)
```

```

{
delay(seg - 200);

digitalWrite(salida8, LOW);

delay(200);

digitalWrite(salida8, HIGH);

pulsos = (pulsos - 1);

Serial.print ("Remaining Pulses = ");

Serial.println (pulsos);

}

Serial.println ("");

Serial.println ("");

Serial.print ("Keeping the Temperature at: ");

Serial.print (tmax); Serial.print (" degrees");

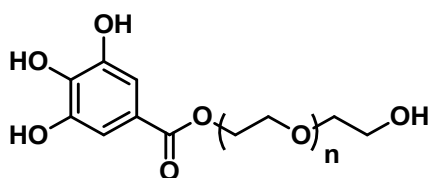
Serial.println ("");

Serial.println ("");

Serial.print("Enter New Parameters [ START TEMP - END TEMP - TIME (min) ]");
}
}

```

### C) Synthesis of PEGylated ligand



In brief, to a solution of polyethylene glycol (Mw: 1500 g/mol, 1 mmol, 1.5 g), gallic acid (Mw: 170 g/mol, 1 mmol, 170 mg) and 4-(dimethylamino) pyridine (Mw: 122 g/mol, 200  $\mu$ mol, 24 mg) in 100 ml of tetrahydrofuran and 10 ml of dichloromethane, in a round-

bottom flask under nitrogen atmosphere, a solution of dicyclohexyl carbodiimide (Mw: 206 g/mol, 5 mmol, 1 g) in tetrahydrofuran was added dropwise. The mixture was stirred overnight at room temperature. The reaction mixture was filtered through a filter paper and the solvents were rota-evaporated.  $^1\text{H}$  NMR spectroscopy confirmed the desired product gallol-PEG-OH.  $^1\text{H}$  NMR (400 MHz,  $\text{CDCl}_3$ )  $\delta$  (ppm): 7.22 (s, 2H), 4.43-4.40 (m, 2H), 3.85-3.45 (m,  $\text{CH}_2$ -PEG, -OH). FTIR peaks ( $\text{cm}^{-1}$ ): 1466 (C-H bend vibration), 1359 (C-H bend vibration), 1341 (C-H bend vibration), 1307 (anti-symmetric stretch vibration), 1268 (C-O stretch vibration), 1238 (C-O stretch vibration), 1092 (C-O-C stretch vibration), 942 (CH out-of-plane bending vibration).

#### **D) Ligand exchange process**

In short, in a glass vial, a solution containing 1.0 ml of NPs (10 g/l of Fe), 1.0 ml of the gallol-PEGn-OH derivative in a concentration of 0.1 M in  $\text{CHCl}_3$  and 50  $\mu\text{l}$  of triethylamine was added. The mixture was ultrasonicated for 1 h and kept 4 h at  $50^\circ\text{C}$ . At this point, it was diluted with 5 ml of toluene, 5 ml of milli-Q water and 10 ml of acetone. Then, it was shaken and the nanoparticles were transferred into the aqueous phase. After that, the aqueous phase was collected in a round-bottom flask and the residual organic solvents were rota-evaporated. Then, the gallol derived MNPs were purified in centrifuge filters with a molecular weight cut-off of 100 kDa at 450 rcf. In each centrifugation, the functionalized MNPs were re-suspended with milli-Q water. The purification step was repeated several times until the filtered solution was clear. After the purification, the gallol derived MNPs were re-suspended in PBS buffer. Finally, to ensure high stable mono-dispersed MNPs, this solution was centrifuged at 150 rcf for 5 min and, it was placed onto a permanent magnet (0.6 T) for 5 min as well.

#### **E) Nuclear Magnetic Resonance Spectroscopy (NMR)**

$^1\text{H}$ -NMR spectra of samples prepared in  $\text{CDCl}_3$  were recorded on an NMR Bruker Ascend 400MHz spectrometer.

#### **F) ICP-HRMS**

IONPs were digested with aqua regia (a mixture of three parts of HCl and one part of  $\text{HNO}_3$ ). Briefly, 2.5 ml of aqua regia were added to 25  $\mu\text{l}$  of a solution of nanoparticles in a volumetric flask. The mixture was left overnight. Then, milli-Q water was added to complete the total volume of 25 ml.

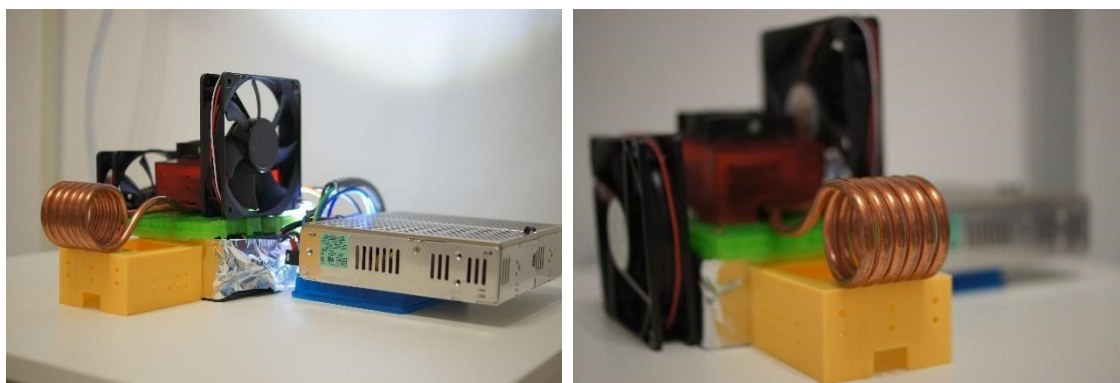
#### **G) Dynamic Light Scattering (DLS)**

The NPs were dispersed in PBS at a concentration of 100 mg/L of Fe. The measurements were done on a cell type: ZEN0118-low volume disposable sizing cuvette, setting 2.420 as refractive index with 90° as the angle of detection. The measurement duration was set as automatic and three as the number of measurements. The general-purpose (normal resolution) model was used for the analysis.

#### **H) Magnetic Characterization**

Sample preparation for magnetic measurement was performed by placing 100  $\mu\text{L}$  of the MNPs suspension into a piece of cotton wool and allowing it to dry at room temperature. The dried wool was then placed inside a gelatine capsule for magnetic characterization. Magnetic measurements were performed in a Quantum Design (USA) MPMS-XL SQUID magnetometer. Field-dependent magnetization was recorded at 300 K in the field ranges between -2000 kA/m and 2000 kA/m.

#### **I) Hyperthermia equipment.**



Picture of the homemade alternating magnetic field (HF-AMF) electromagnetic inductor.

#### **J) *In vitro* longitudinal and transversal relaxivities ( $r_1$ and $r_2$ )**

Both  $T_1$  and  $T_2$  relaxation times were obtained using solutions of magnetic NPs in PBS with Fe concentrations ranging between 0.125 and 2 mM.  $T_1$  was determined using an inversion-recovery sequence, and  $T_2$  using the Carl-Purcell-Meiboom-Gill (CPMG) spectroscopy sequence. The relaxivities ( $r_1$  and  $r_2$ ), were calculated from the slope of the linear fit of the relaxation rate ( $1/T_X$ ) versus Fe concentration.

#### **K) Cytotoxicity evaluation**



*Cell morphology studies and “live-dead” assay.* The N13 cells were plated at a density of  $1 \times 10^4$  cells/well in a 96-well plate at 37 °C in 5% CO<sub>2</sub> atmosphere (200 µl per well, number of repetitions = 5). After 24 h of culture, the medium inside the wells was replaced with fresh medium containing the magnetic nanoparticles in varying concentrations from 0.1 µg/ml to 100 µg/ml. Similarly, for the cytotoxicity assays, after 24 h, Ethanol 20% was added to the positive control wells. After 15 min, all the wells were stained with DAPI (4',6-Diamidino-2-phenylindole) (dilution 1:3000) to label nuclei in all cells, although with stronger labeling in live cells, and TO-PRO-3 Iodine to only label dead cells (dilution 1:1000). The cell morphology images were acquired using a Perkin Elmer Operetta High Content Imaging System with a 20x LWD 0.45 NA air objective lens. 5 well replicas for each condition were analyzed with 10 random image fields captured per well. For each field, fluorescence images for DAPI and TO-PRO-3, plus a brightfield image, were captured. Cell mortality percentages were calculated automatically by Operetta Harmony software, whereby all nuclei (dead and alive) were identified from the DAPI staining, and the percentage of dead cells was then determined by the number of nuclei also possessing high levels of TO-PRO-3 staining.

*MTT assay.* In short, the N13 cells were plated at a density of  $1 \times 10^4$  cells/well in a 96-well plate at 37 °C in 5 % CO<sub>2</sub> atmosphere (200 µl per well, number of repetitions = 5). After 24 h of culture, the medium in the wells was replaced with fresh medium containing magnetic nanoparticles in varying concentrations from 0.1 µg/ml to 100 µg/ml. After 24 h, the supernatant of each well was replaced by 200 µl of fresh medium with 3-[4,5-dimethylthiazol-2-yl]-2,5-diphenyl tetrazolium bromide (MTT) (0.5 mg·ml<sup>-1</sup>). After 2 h of incubation at 37 °C and 5 % CO<sub>2</sub>, the medium was removed, the formazan crystals were solubilized with 200 µl of DMSO, and the solution was vigorously mixed to dissolve the reacted dye. The absorbance of each well  $[Abs]_{well}$  was read on a microplate reader (Dynatech MR7000 instruments) at 550 nm. The relative cell viability (%) and its error related to control wells containing cell culture medium without nanoparticles were calculated by the equations:

$$RCV(\%) = \left( \frac{[Abs]_{test} - [Abs]_{Pos.Ctrl.}}{[Abs]_{Neg.Ctrl.} - [Abs]_{Pos.Ctrl.}} \right) \times 100$$

$$Error(\%) = RCV_{test} \times \sqrt{\left( \frac{\sigma_{test}}{[Abs]_{test}} \right)^2 + \left( \frac{\sigma_{Ctrl}}{[Abs]_{Ctrl.}} \right)^2}$$

where  $\sigma$  is the standard deviation.

Triton X-100 was added to the positive control wells.

### **L) MRI studies**

*Experiments in mice.* High-resolution T<sub>2</sub>-weighted images were acquired using a turbo-RARE sequence with respiratory gating (TE = 16 ms, TR = 1000 ms, 4 averages, 156  $\mu$ m in-plane resolution and 1 mm slice thickness).

### **M) Histology**

The tissues were fixed in 4% formaldehyde (Panreac, pH 7 buffered) for 48 h, changing the 4% formaldehyde after 24 h. Then, the samples were dehydrated through graded ethanol and embedded in paraffin (temperature 56° C for 2 h under stirring and vacuum). The detailed procedures are described below.

Haematoxylin and Eosin (H&E): paraffin-embedded samples were sectioned at 7  $\mu$ m thickness, then deparaffinized, rehydrated and stained with H&E, and then dehydrated in ascending concentrations of ethanol, cleared in xylene, and mounted on commercial glass slides.

## **2. Results**

### **A) Characterization**

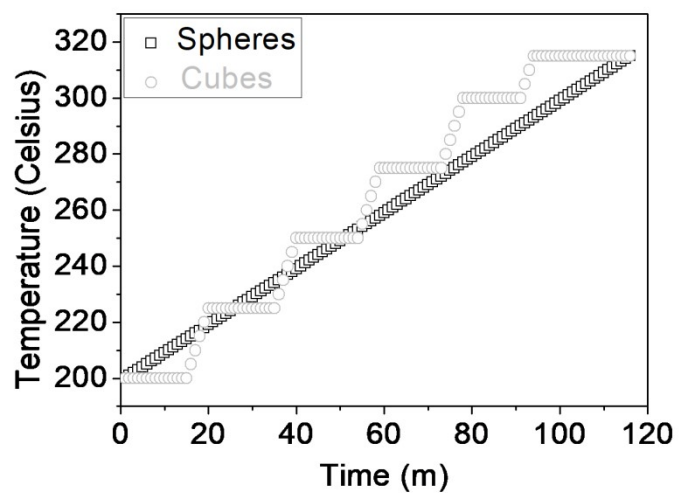


**Figure S1.** Representation of ramp temperature: spheres (black) and cubes (grey).

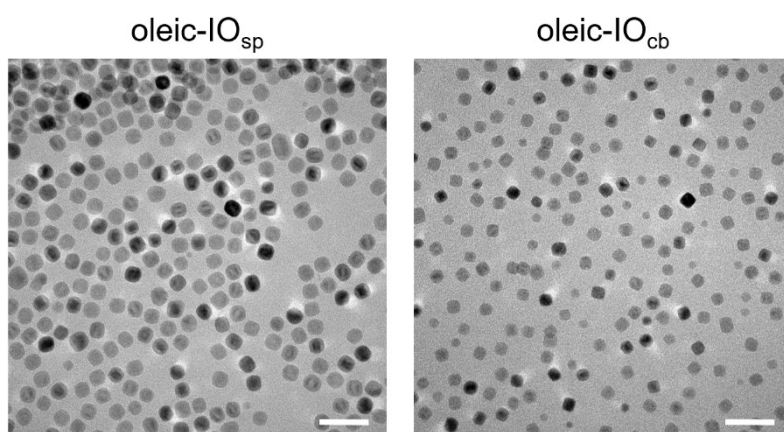


**Figure S2.** TEM images of oleic acid capped. Scale bar corresponds to 50 nm.

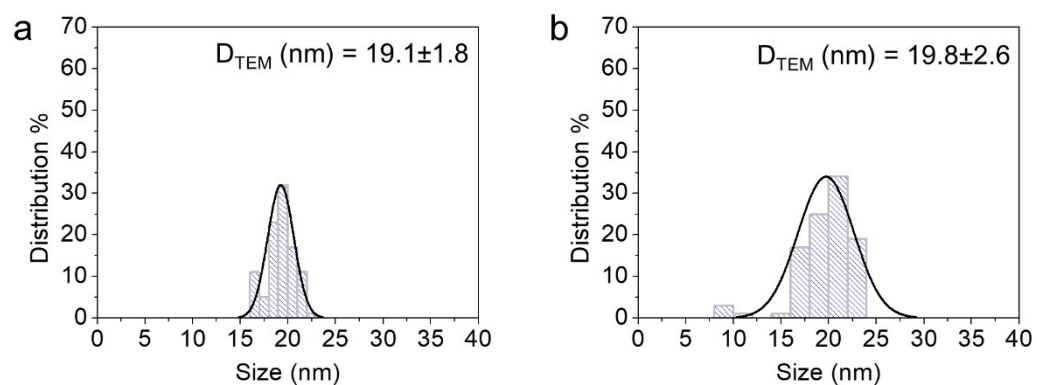


**Figure S3.** Representative size histogram of oleic-IO<sub>sp</sub> (left) and oleic-IO<sub>cb</sub> (right). Sizes were calculated from at least 100 nanoparticles.

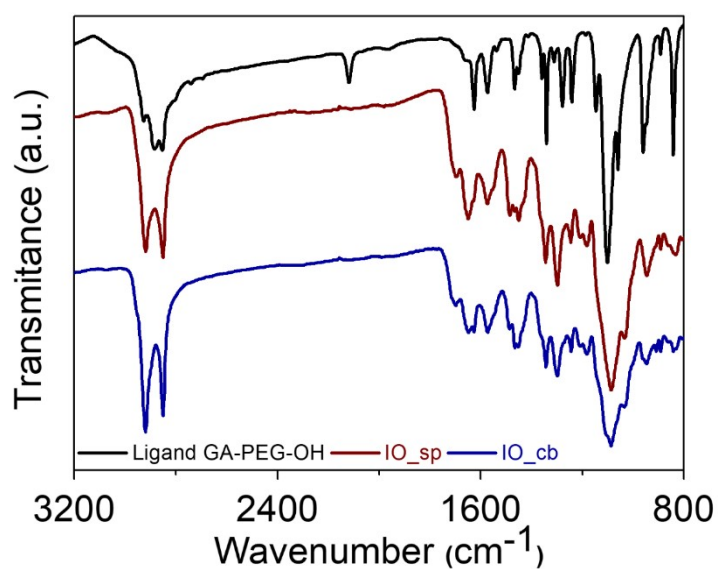


**Figure S4.** FTIR spectra of PEGylated ligand (black), IO<sub>sp</sub> (red) and IO<sub>cb</sub> (blue) after the ligand exchange process

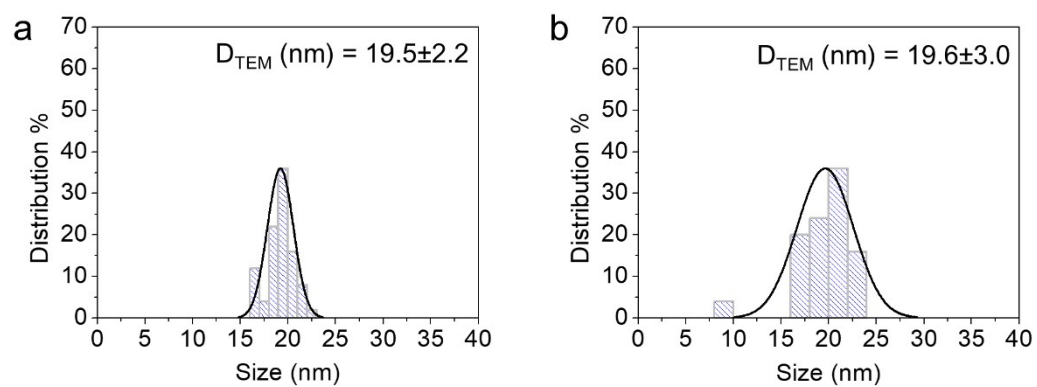


**Figure S5.** Representative size histogram of  $IO_{sp}$  (left) and  $IO_{cb}$  (right). Sizes were calculated from at least 100 nanoparticles.

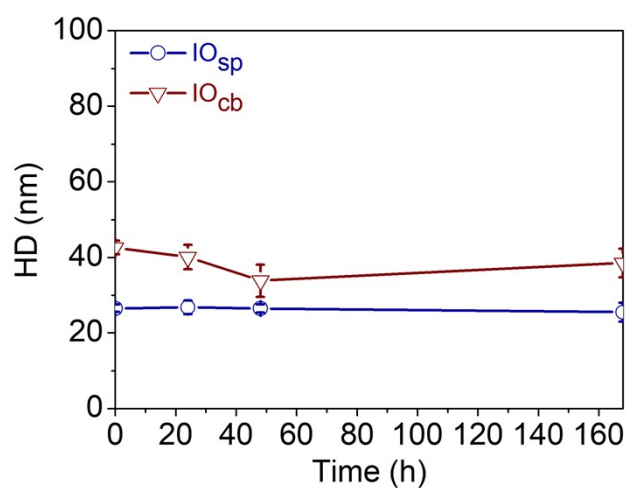


**Figure S6.** Measurement of the HDs of the different functionalized IONPs over time.

**B) *In vitro* longitudinal relaxivities**

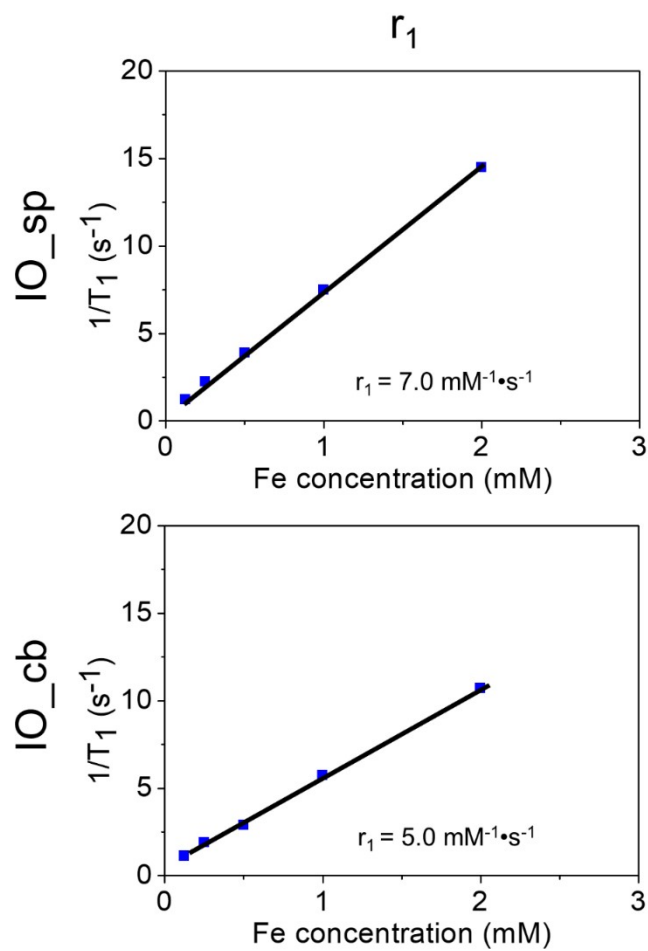


**Figure S7.** Plot of  $1/T_1$  over Fe concentration of nanoparticles (right): longitudinal relaxivity calculated at 1.44 T for  $IO_{sp}$  (top) and  $IO_{cb}$  (bottom).

### C) Cytotoxicity evaluation

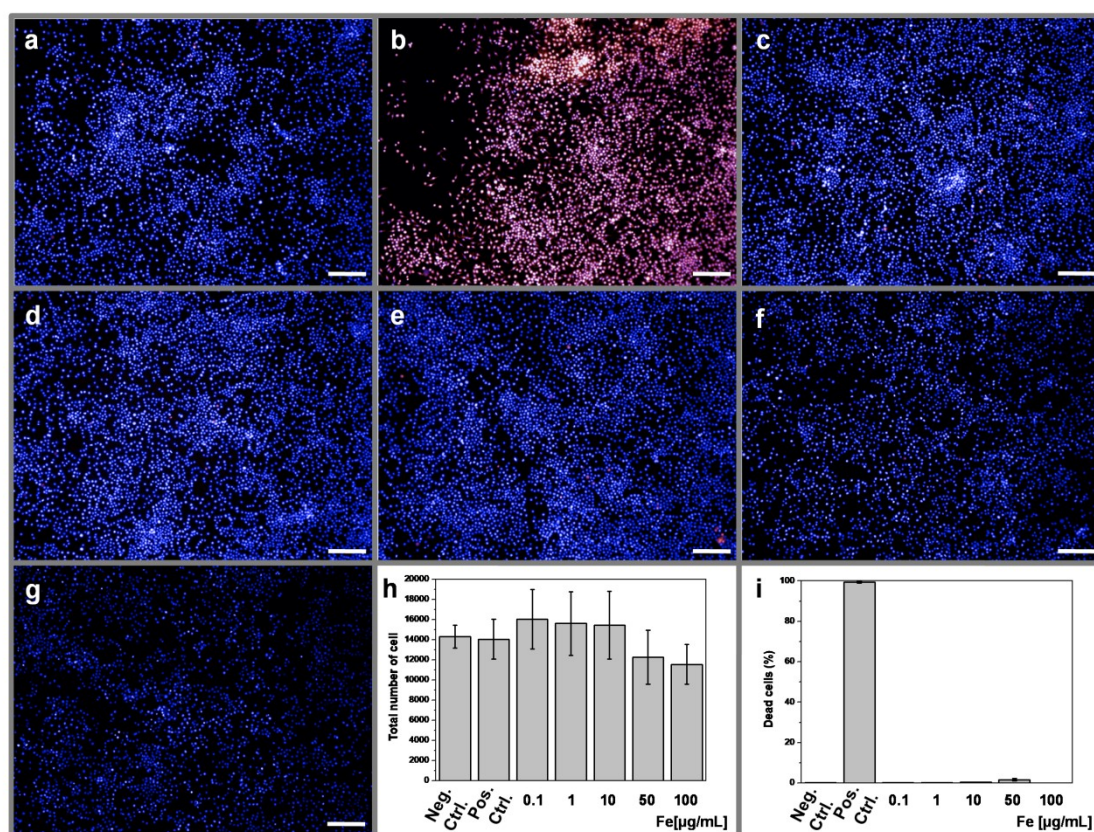


**Figure S8.** Representative images of the cultured cell: a) Negative control, b) Positive control, c)-g) cells exposed to IO<sub>sp</sub> concentration from 0.1 μg/ml to 100 μg/ml. The images show the merge of DAPI (blue) and TO-PRO-3 Iodine (red) images. Scale bar is 100 μm. h) Total number of cells per well exposed to increasing concentration of IO<sub>sp</sub>. i) Percentage of dead cells exposed to increasing concentration of IO<sub>sp</sub>.

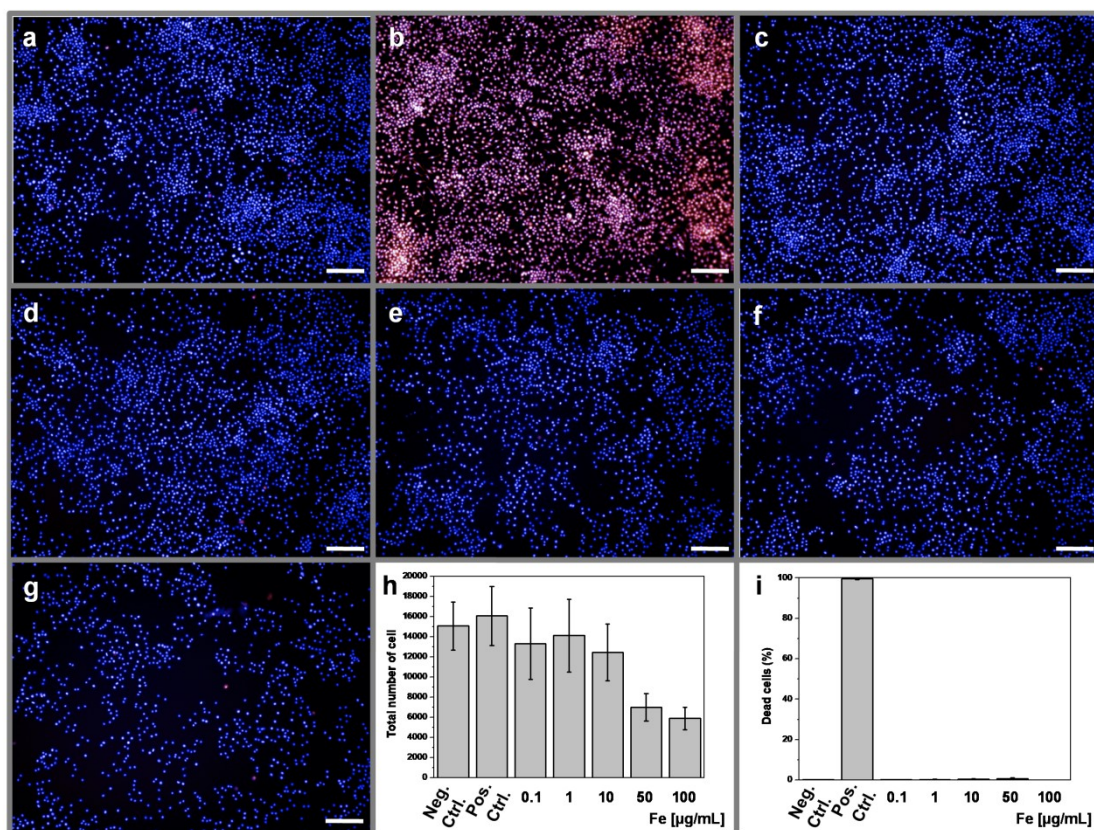


**Figure S9.** Representative images of the cultured cell: a) Negative control, b) Positive control, c)-g) cells exposed to IO<sub>cb</sub> concentration from 0.1 μg/ml to 100 μg/ml. The images show the merge of DAPI (blue) and TO-PRO-3 Iodine (red) images. Scale bar is 100 μm. h) Total number of cells per well exposed to increasing concentration of IO<sub>cb</sub>. i) Percentage of dead cells exposed to increasing concentration of IO<sub>sp</sub>.



## D) Biodistribution MRI studies in tumor-bearing mice after I.V. administration

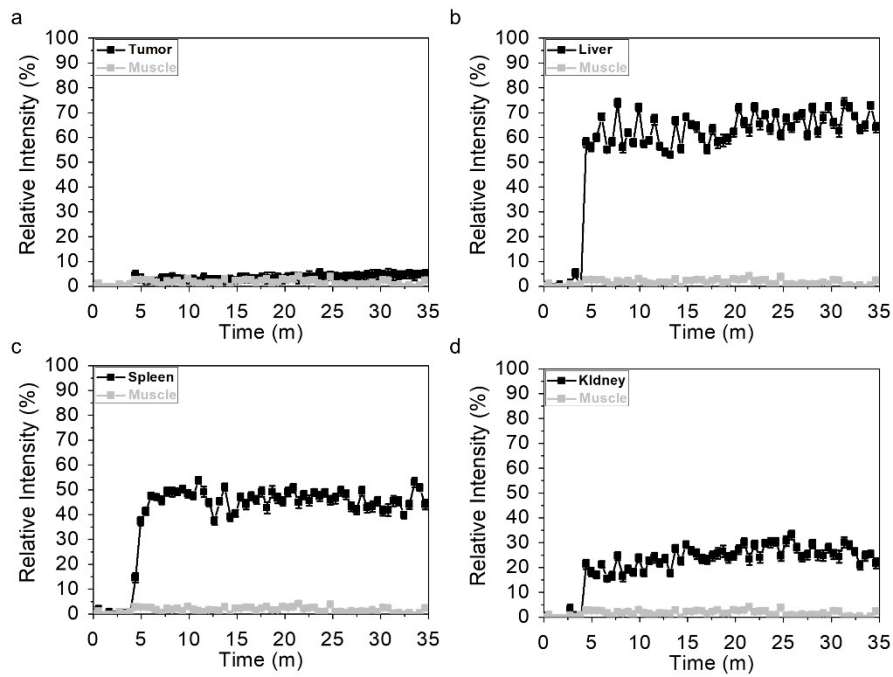


**Figure S10.** *In vivo* time courses of: a) tumor, b) liver, c) spleen and d) kidneys of mice after being intravenously injected with  $IO_{sp}$ . Muscle was used as control tissue (grey in all cases).

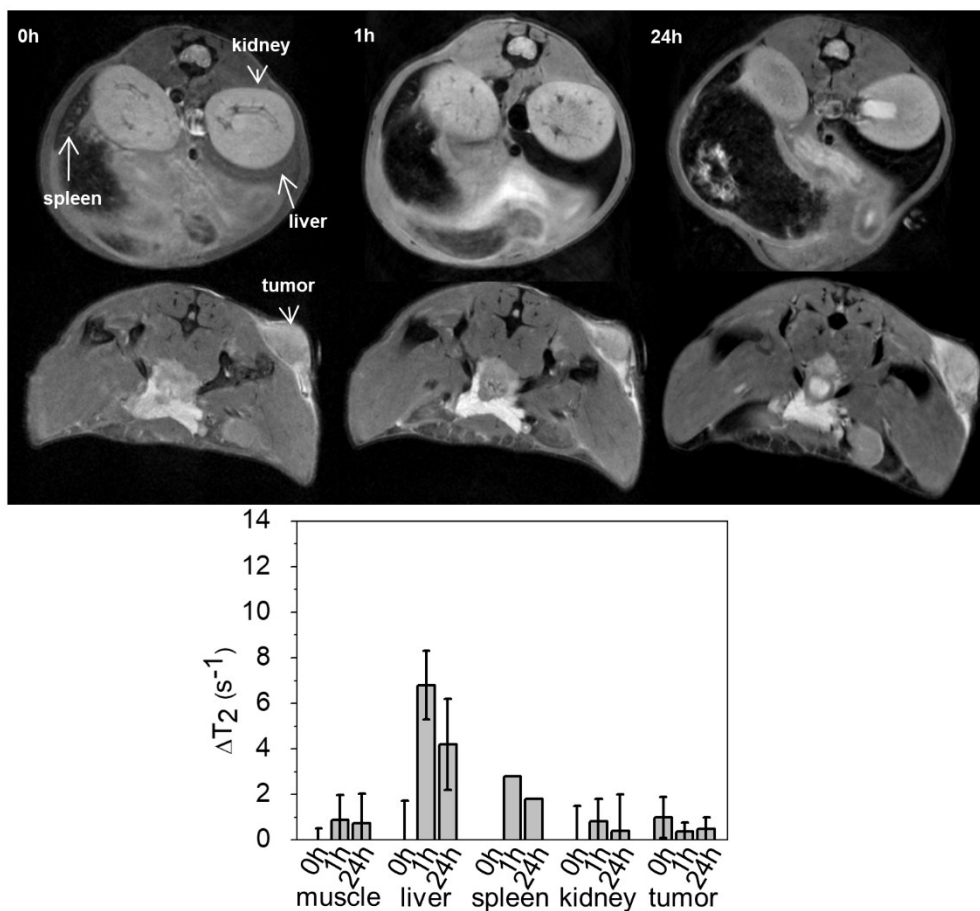


**Figure S11.** Top: Representative T<sub>2</sub>-weighted MR images at different experimental time points after the intravenous injection of IO<sub>sp</sub>. Bottom:  $\Delta T_2$  values of different organs at 1h and 24h after the intravenous injection of IO<sub>sp</sub>. The average values were obtained by performing 3 experiments.

### E) MRI of magnetic hyperthermia process

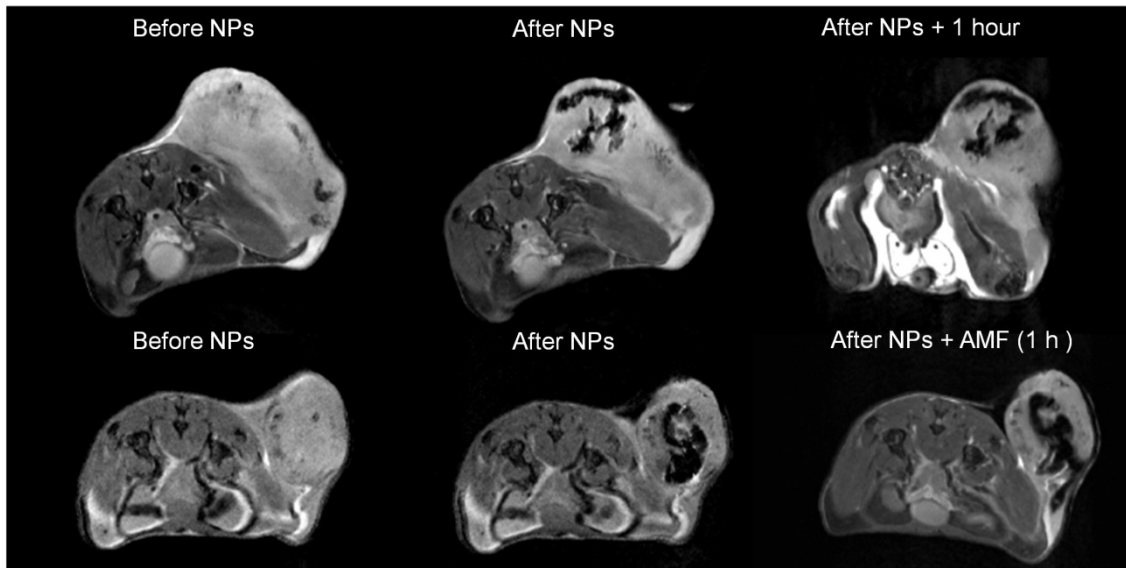


**Figure S12.** Representative MR images of tumor-bearing mice before (left) and after intratumoral injection of  $\text{IO}_{\text{sp}}$  (centre). MR images of tumor-bearing mice 1 hour after  $\text{IO}_{\text{sp}}$  injection (top right) and 1 hour under AMF after  $\text{IO}_{\text{sp}}$  injection (bottom right).

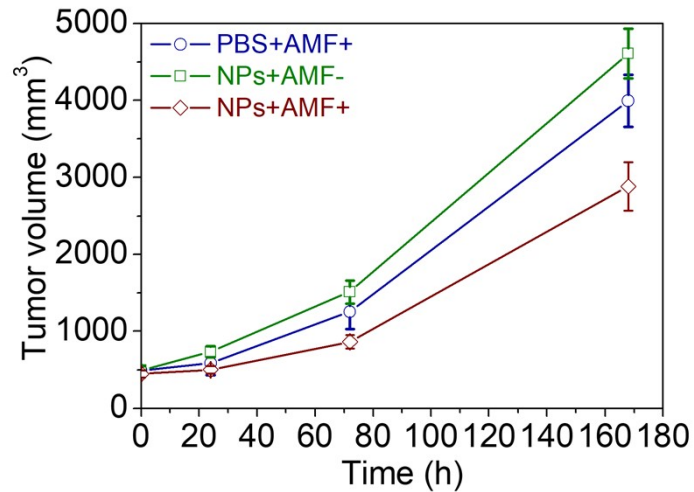


**Figure S13.** Tumor volume evaluation by  $T_2$ -weighted MRI images. NPs were intravenously injected at time = 0h.

## F) Histology

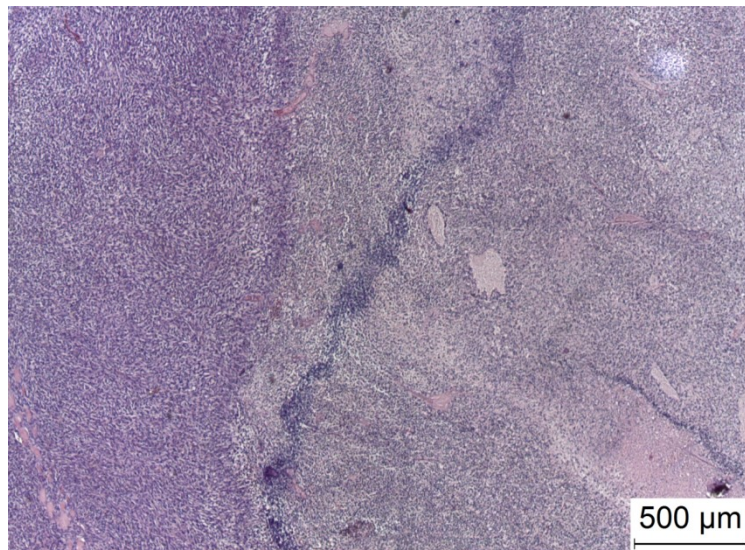


**Figure S14.** Representative histology section of tumor-bearing mice 7 days after the intratumoral injection of PBS.